Vol 18 No 7, July 2009
1674-1056/2009/18(07)/2788-06

Chinese Physics B

© 2009 Chin. Phys. Soc.
and IOP Publishing Ltd

Dispersion effect in optical microscopy systems with a supersphere solid immersion lens*

Zhang Yao-Ju(张耀举)† and Zhuang You-Yi(庄友谊)

College of Physics and Electronic Information, Wenzhou University, Wenzhou 325035*, China*

(Received 15 December 2008; revised manuscript received 20 December 2008)

This paper studies the dispersion effect of the supersphere solid immersion lens (SIL) on a near field optical microscopy system by using the vector diffraction theory. Results show that when a real non-monochromatic beam illuminates a supersphere SIL microscopy, the dispersion effect of the SIL has an important influence on the image quality. As the wavelength bandwidth of the non-monochromatic beam increases, the size of the focused spot increases and its intensity decreases in near-field microscopy systems with a supersphere SIL.

Keywords: dispersion, supersphere solid immersion lens, microscopy
PACC: 4230H, 4230F, 4225F, 4280T

1. Introduction

For conventional optical microscopy, the refractive index of air in the object space is unity, which limits the numerical aperture (NA) to unity and consequently limits the lateral resolution to $\lambda_0/2$, where λ_0 is the free space wavelength of light. The resolution of the conventional optical microscope can be improved only by a small extent by using superresolving diffractive optical elements.[1−4] The near-field solid immersion lens (SIL) technique, which is different from the near-field scanning optical microscopy,[5,6] is not by definition limited to point-by-point imaging but can offer excellent spatial resolution over an extended field by placing additional refraction or reflection elements in the optical near-field of the surface of an object.[7−13]

Since Mansfield and Kino first proposed and demonstrated a hemisphere SIL microscope to clearly resolve 100 nm lines and spaces in photoresist,[7] the SIL technique has been developed as a path to achieve higher optical data densities on the plane of the recording layer[8] or to improve the collection efficiency in fluorescence microscopy[14] and in semiconductor single-photon emitter of light.[15] The SIL technique has also been applied in surface plasmon microscopy[16] and near-field photolithography.[17] Recently, Ippolito *et al* used SILs to achieve very high subsurface imaging resolution in silicon wafers.[10] More recently, Zhang and Bai[18] applied the SIL technique to the proposed high-density all-optical magnetic recording.

In applications, two types of SILs are developed which use spherical-only surfaces. One type of SIL is a hemisphere lens with the flat surface in proximity to the recording layer or to the microscopy specimen.[7] The other type of SIL is a supersphere SIL with its flat rear surface in proximity to the recording layer or to the microscopy specimen.[8] To further improve the resolution of SIL microscopy systems or increase the focal depth in near-field SIL optical data storage systems, some amplitude and/or phase filters have been added in SIL microscopy systems.[19−23]

In theory, previous analyses and calculations for the transmitted field of SILs are based on the monochromatic light illuminating the SIL systems and the dispersion of SILs is not considered. This paper shows that the non-monochromaticity of the incident beam and the dispersion effect in a supersphere SIL have an important influence on the lateral resolution and intensity of the focused spot.

2. Aberration function of a supersphere SIL

It is well known that to achieve high recording density or high resolution, materials with high refrac-

*Project supported by National Natural Science Foundation of China (Grant No 60777005).
†Corresponding author. E-mail: zhangyaoju@sohu.com

tive index, such as Si and GaP, are usually used. The refractive index of these materials varies with wavelength generally. Even if the refractive index is insensitive to wavelength for some glass materials within the visible light spectrum, weak dispersion has an important influence on resolution of a supersphere SIL system, because the structure of a supersphere SIL is related to its refractive index. In this section, the aberration function of a supersphere SIL is derived.

Figure 1 shows the imaging parameters for a supersphere SIL. In practice, the incident beam on the SIL is usually non-monochromatic. Assume that the

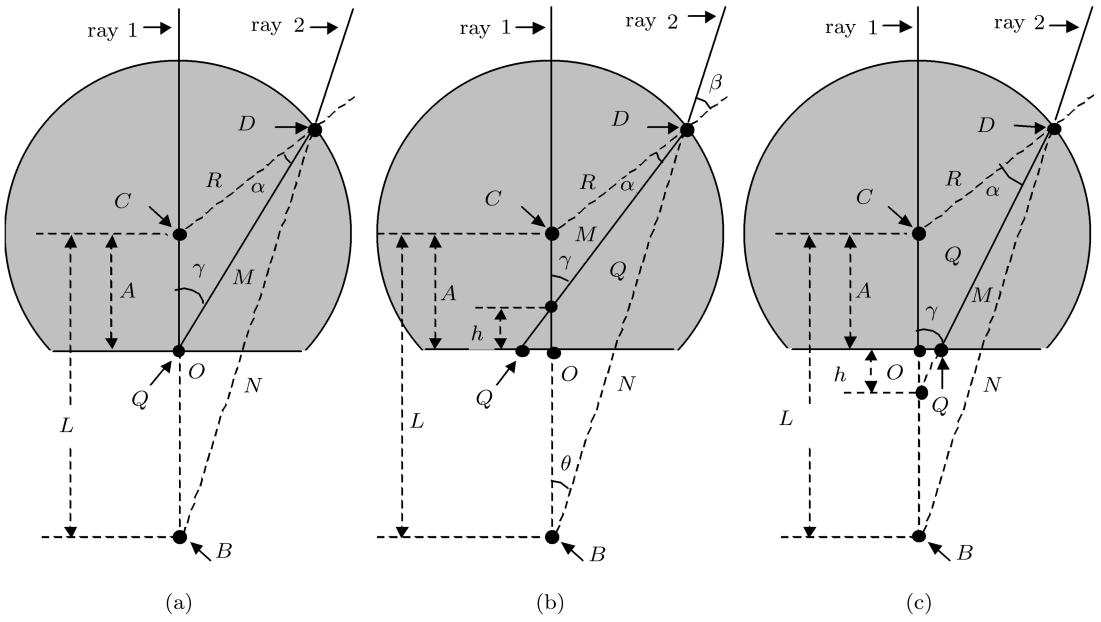


Fig.1. Imaging parameters for a supersphere lens and dispersion, (a) $n(\lambda) = n(\lambda_c)$, (b) $n(\lambda) > n(\lambda_c)$ and (c) $n(\lambda) < n(\lambda_c)$.

wavelength of the incident beam is in the range from $\lambda_c - w/2$ to $\lambda_c + w/2$, where λ_c is the central wavelength and w is the wavelength bandwidth. For a SIL surface microscopy, one can design the structure of the SIL and adjust its position in the image system so that incident lights at the central wavelength of $\lambda = \lambda_c$ are aplanatically focused at point O on the planar surface of the SIL, as shown in Fig.1(a). Ray 1 passing through the centre (point C) of the sphere arrives at point O and ray 2 passing through the spherical boundary at point D arrives at point Q. (Q and O superpose together for $n(\lambda) = n(\lambda_c)$, but they do not for $n(\lambda) \neq n(\lambda_c)$, see Fig.1). B is the position of the virtual focus. Ray 1 is defined as the reference ray. Ray 2 forms an angle γ, with respect to ray 1, and an angle of α, with respect to the line from C to D. The distances from Q to D and from B to D are defined as M and N, respectively. According to the geometric relationships in Fig.1, M and N can be obtained as

$$M = (A-h)\cos\gamma + \sqrt{R^2 - (A-h)^2\sin^2\gamma} + h/\cos\gamma, \tag{1}$$

$$N = \sqrt{R^2 + L^2 + 2L\left[\cos\gamma\sqrt{R^2 - (A-h)^2\sin^2\gamma} - (A-h)\sin^2\gamma\right]}, \tag{2}$$

where

$$h=\begin{cases}0, & \text{for } n(\lambda)=n(\lambda_c),\\ A-\dfrac{R\sin\alpha}{\sin\gamma}, & \text{for } n(\lambda)>n(\lambda_c),\\ -A+\dfrac{R\sin\alpha}{\sin\gamma}, & \text{for } n(\lambda)<n(\lambda_c),\end{cases} \tag{3}$$

$$\begin{aligned}\alpha&=\arcsin\left[\frac{L}{n(\lambda)R}\sin\theta\right],\\ \beta&=\arcsin\left[\frac{L}{R}\sin\theta\right],\\ \gamma&=\theta+\beta-\alpha.\end{aligned} \tag{4}$$

The optical path length (OPL) from Q to D and then to B is

$$\mathrm{OPL}(A,L,\gamma,\lambda)=n(\lambda)M-N\,. \tag{5}$$

Then the wave aberration function is expressed as

$$\psi(\lambda)=k[\mathrm{OPL}(A,L,\gamma,\lambda)-\mathrm{OPL}(A,L,0,\lambda)]. \tag{6}$$

After some algebraic calculations, we obtain the resulting aberration function:

$$\begin{aligned}\psi(\lambda)=k\Bigg\{&R[1-n(\lambda)]+n(\lambda)(A-h)(\cos\gamma-1)+L+n(\lambda)\sqrt{R^2-(A-h)^2\sin^2\gamma}\\ &+n(\lambda)h\left(\frac{1-\cos\gamma}{\cos\gamma}\right)-\sqrt{R^2+L^2+2L\left[\cos\gamma\sqrt{R^2-(A-h)^2\sin^2\gamma}-(A-h)\sin^2\gamma\right]}\Bigg\}.\end{aligned} \tag{7}$$

Specially, for the light of $\lambda=\lambda_c$, the aberration function is

$$\begin{aligned}\psi(\lambda_c)=k\Bigg\{&R[1-n(\lambda_c)]+n(\lambda_c)A(\cos\gamma-1)+L+n(\lambda_c)\sqrt{R^2-A^2\sin^2\gamma}\\ &-\sqrt{R^2+L^2+2L\left[\cos\gamma\sqrt{R^2-A^2\sin^2\gamma}-A\sin^2\gamma\right]}\Bigg\}.\end{aligned} \tag{8}$$

It is found from Eq.(8) that in the aplanatic solution for the central wavelength of the beam, A and L are equal to $R/n(\lambda_c)$ and $Rn(\lambda_c)$, respectively. In this condition, the lights departing from the central wavelength produce the aberration on the planar surface of the SIL, which is determinated by Eq.(7). In the following calculations, the fused quartz glass is chosen as the material of the SIL with refractive index function[24]

$$n(\lambda)=\sqrt{2.978645+\frac{0.008777898}{\lambda^2-0.010609}+\frac{84.06224}{\lambda^2-96.00000}}. \tag{9}$$

Figure 2(a) plots the dependence of the refractive index on the wavelength. It is clear that the dispersion of the refractive index with wavelength λ is very small in the range of λ from 509 nm to 519 nm. However, it

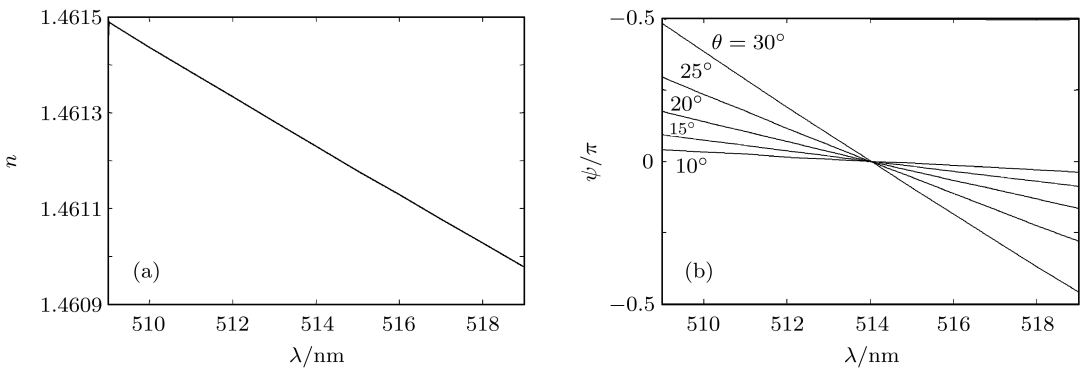


Fig.2. Dispersion of the refractive index: (a) for a fused quartz glass and the aberration function; (b) for the supersphere SIL with the radius of $R=1$ mm. The fused quartz glass SIL is designed aplanatically for central wavelength $\lambda_c=0.514$ μm of the beam.

is this small dispersion that produces a non-neglectable aberration in the supersphere SIL, which is shown in Fig.2(b). The SIL in the figure is designed aplanatically for central wavelength $\lambda_c = 514$ nm of the beam and its radius is $R = 1$ mm. It is seen from Fig.2(b) that the absolute value of the aberration function increases as the wavelength and incident angle increase, and when $\theta = 30°$ the maximum phase difference is close to $\pi/2$, which has an influence on the resolution of the SIL microscopy system.

3. Optical field distribution of the SIL microscopy system

The system considered consists of an ideal converging lens (L_1) with high NA and a supersphere SIL, as shown in Fig.3. The SIL, surrounded by air, is close to the focus of the converging lens L_1. The origin O is at the focus of the system. The thickness of the supersphere SIL is $R + A$, where R is the radius of the sphere. The distance between the Gaussian focus of the converging lens and the centre of the SIL is $L(L + R < f_0$, f_0 is the focal length of the converging lens). We let $A = R/n(\lambda_c)$ and $L = Rn(\lambda_c)$ so that the lights with the central wavelength are aplanatically focused at the focus. Consideration of a high NA lens requires a model of diffraction defined by vector field theory, rather than scalar field theory. An angular spectrum of plane waves method, as described by Richard and Wolf[25] and developed by Török *et al*[26] can be used to find the electric field at any point near the focus, with cylindrical coordinates (ρ_c, z_c, ϕ_c). We assume that the lens is illuminated by a collimated radially-polarized plane wave beam. The electric field on the focal plane can be obtained as Ref.[19]

$$E_\rho(\lambda) = \mathrm{i}\int_0^{\theta_m} t_\mathrm{p}\xi(\lambda)\sqrt{\cos\theta}\sin\theta\sin\Theta\exp[\mathrm{i}\psi(\lambda)]J_1[kn(\lambda)\rho_C\sin\gamma]\mathrm{d}\theta,$$
$$E_z(\lambda) = 2\int_0^{\theta_m} t_\mathrm{p}\xi(\lambda)\sqrt{\cos\theta}\sin\theta\sin\Theta\exp[\mathrm{i}\psi(\lambda)]J_0[kn(\lambda)\rho_C\sin\gamma]\mathrm{d}\theta, \quad (10)$$

where E_ρ and E_z are the transverse and longitudinal elements of electric fields, respectively, in cylindrical coordinates, J_n is the nth Bessel function of the first kind, θ_m is the maximum converging angle of the lens L_1, t_p is the Fresnel transmission coefficient of the SIL, and

$$\Theta = \theta + \beta + \eta - \alpha - \gamma,$$
$$\eta = \arcsin(n\sin\gamma). \quad (11)$$

In Eq.(10) ξ (λ) is the distribution function of the incident beam with wavelength λ. Without loss of generality, we assume that ξ (λ) is a Gaussian distribution with wavelength λ

$$\xi(\lambda) = \exp\left[\frac{(\lambda-\lambda_c)^2}{(w/2)^2}\right], \quad (12)$$

where λ_c is the central wavelength and w is the wavelength bandwidth.

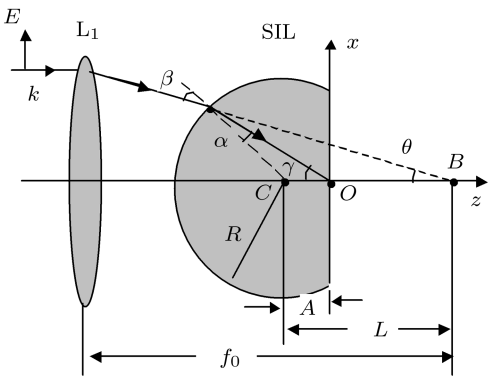


Fig.3. Schematic drawing for microscopy system with a supersphere SIL.

The intensity of the light in the transmitted field is expressed as

$$I = \frac{1}{w}\int_{\lambda_0-w/2}^{\lambda_0+w/2}\left[|E_\rho(\lambda)|^2 + |E_z(\lambda)|^2\right]\mathrm{d}\lambda. \quad (13)$$

Figure 4 shows the normalized intensity distributions in the focal plane of a supersphere SIL microscopy system illuminated by radially-polarized beams with different wavelength bandwidths. The supersphere SIL made of fused quartz glass material is designed aplanatically for central wavelength $\lambda_c = 0.514$ μm of the beam. From the figure it can be seen that the dispersion effect of the SIL enlarges the size of the focused spot, in comparison with the case in the monochromatic incident beam ($w = 0$). We define the fully-width at half maximum (FWHM) of the size of spot. Generally, as the wavelength bandwidth increases, FWHM of spot increases but the intensity of spot decreases, as shown in Fig.5.

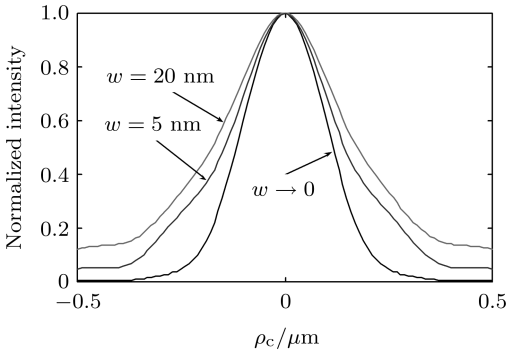


Fig.4. Normalized intensity distribution in the focal plane of a supersphere SIL system illuminated by non-monochromatic beams with different wavelength bandwidths. The fused quartz glass SIL with radius 1.6 mm is designed aplanatically for central wavelength $\lambda_c = 0.514$ μm of the beam.

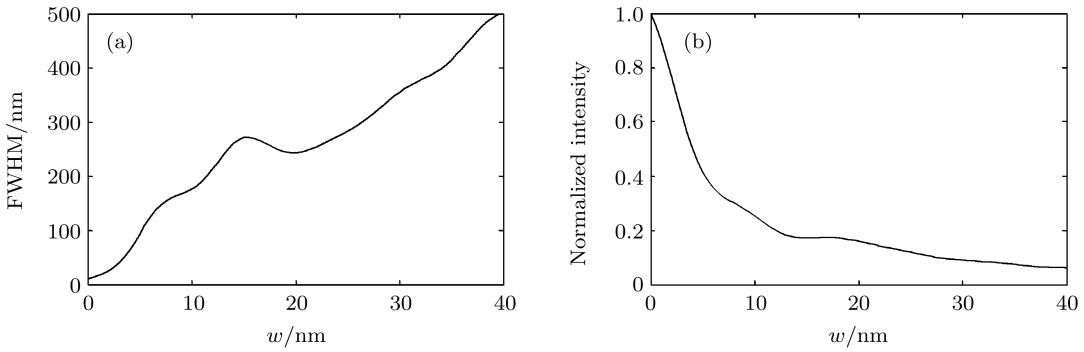


Fig.5. The size (FWHM) of the focused spot (a) and its normalized intensity (b) as a function of the wavelength bandwidth of the beam incident on the supersphere SIL system.

4. Conclusions

In practice, light beams illuminating optical microscopy systems usually are non-monochromatic ones with certain wavelength bandwidth, rather than an ideal monochromatic beam. In this paper, the aberration function of a supersphere SIL with dispersion effect is first derived and then the expression for the transmitted field is given for a supersphere SIL microscopy system illuminated by a non-monochromatic radially-polarized beam. The numerical results show that the dispersion effect in the SIL material results in the degeneration of the image quality in supersphere SIL microscopy systems.

References

[1] Jia J, Zhou C and Liu L 2003 *Opt. Commun.* **228** 271
[2] Zhou S and Zhou C 2004 *Opt. Lett.* **29** 2746
[3] Luo H and Zhou C 2004 *Appl. Opt.* **43** 6242
[4] Zhang Y 2007 *Opt. Commun.* **274** 37
[5] Betzig E, Trautman J K, Harris T D, Weiner J S and Kostelak R L 1991 *Science* **251** 1468
[6] Wang Q, Xu J Q, Wu J and Li Y J 2003 *Acta Phys. Sin.* **52** 298 (in Chinese)
[7] Mansfield S M and Kino G S 1990 *Appl. Phys. Lett.* **57** 2615
[8] Terris B D, Mamin H J and Ruger D 1994 *Appl. Phys. Lett.* **65** 368
[9] Terris B D, Mamin H J and Rugar D 1996 *Appl. Phys. Lett.* **68** 141
[10] Ippolito S B, Thorne S A, Eraslan M G, Goldberg B B and Ünlü M S 2004 *Appl. Phys. Lett.* **84** 4529
[11] Michaels C A 2007 *Appl. Phys. Lett.* **90** 121131

[12] Zhang Y 2007 *J. Opt. Soc. Am.* A **24** 211
[13] Zhang Y, Chen J and Ye X 2007 *Opt. Commun.* **269** 271
[14] Yoshita Y, Koyama K, Baba M and Akiyama H 2002 *J. Appl. Phys.* **92** 862
[15] Zwiller V and Björk G 2002 *J. Appl. Phys.* **92** 660
[16] Zhang J, See C W, Somekh M G, Pitter M C and Liu S G 2004 *Appl. Phys. Lett.* **85** 5451
[17] Ghislain L P, Elings V B, Crozier K B, Manalis S R, Minne S C, Wilder K, Kino G S and Quate C F 1999 *Appl. Phys. Lett.* **74** 501
[18] Zhang Y and Bai J 2008 *Phys. Lett.* A **372** 6294
[19] Helseth L E 2001 *Opt. Commun.* **191** 161
[20] Zheng C W and Dai Y X 2005 *Chin. Phys.* **14** 1585
[21] Zhang Y, Xiao H and Zheng C 2004 *New J. Phys.* **6** 75
[22] Liu C and Park S H 2004 *Opt. Lett.* **29** 1742
[23] Zhang Y and Ye X 2007 *Appl. Phys.* B **86** 97
[24] Rodney W S and Spindler R J 1954 *J. Opt. Soc. Am.* **44** 677
[25] Richard B and Wolf E 1959 *Proc. Roy. Soc. Ser.* A **253** 358
[26] Török P , Varga P, Laczik Z and Booker G R 1995 *J. Opt. Soc. Am.* A **12** 325